Liquid Crystals
Publication details, including instructions for authors and subscription information:
http://www.informaworld.com/smpp/title~content=t713926090

Twist deformation in anticlinic antiferroelectric structure in smectic B_2 imposed by the surface anchoring

Lubor Lejček[a]; Vladimíra Novotná[a]; Milada Glogarová[a]
[a] Institute of Physics, Academy of Sciences of the Czech Republic, 182 21 Prague 8, Czech Republic

To cite this Article Lejček, Lubor , Novotná, Vladimíra and Glogarová, Milada(2008) 'Twist deformation in anticlinic antiferroelectric structure in smectic B_2 imposed by the surface anchoring', Liquid Crystals, 35: 1, 11 — 19
To link to this Article: DOI: 10.1080/02678290701744553
URL: http://dx.doi.org/10.1080/02678290701744553

Liquid Crystals, Vol. 35, No. 1, January 2008, 11–19

Taylor & Francis
Taylor & Francis Group

Twist deformation in anticlinic antiferroelectric structure in smectic B_2 imposed by the surface anchoring

LUBOR LEJČEK*, VLADIMÍRA NOVOTNÁ and MILADA GLOGAROVÁ
Institute of Physics, Academy of Sciences of the Czech Republic, Na Slovance 2, 182 21 Prague 8, Czech Republic

(*Received 26 July 2007; accepted 12 October 2007*)

A simplified model is used to estimate the energies of observed structures in the smectic B_2 phase composed of bent-shaped molecules. An approximate twist solution connecting anticlinic antiferroelectric structure in the sample bulk with synclinic ferroelectric order induced at the sample surfaces by anchoring is proposed and the elastic and anchoring energies of this structure are determined. It is shown that uniform, twisted and partly twisted (mixed) anticlinic antiferroelectric structures can coexist with nearly the same energies.

1. Introduction

Smectic phases composed of molecules with bent-shaped cores (see, e.g., [1–12]) have been studied intensively recently. The reason for such an interest is their ability to form dipolar ordering, which originates from a combination of molecular tilt (with respect to the layer normal) and molecular dipole moment orientations. Such a combination gives a variety of chiral structures, which is also a consequence of their molecular biaxiality. The dipolar ordering of these smectic phases led to the observed textures in [1–12].

In [9–12] observations of textures that reflect twisted structures in the B_2 (denoted also as Sm-CP) phase were reported. Without an applied electric field, an anticlinic antiferroelectric structure usually occurs. However, when the sample is cooled slowly, domains of twisted structure are observed together with domains of uniform anticlinic antiferroelectric structure (SmC_AP_A) [12]. The twisted structure in [12] was proposed as the connection of anticlinic antiferroelectric (SmC_AP_A) structure in the sample bulk with synclinic ferroelectric (SmC_SP_F) structure imposed by surface anchoring.

In the present contribution we discuss the possible twisted structures that might occur in the B_2 phase. Let us suppose that the surface anchoring prefers the surface synclinic ferroelectric structure. Then the anticlinic antiferroelectric bulk structure can be mediated to surface synclinic ferroelectric order by molecular rotation in one layer while molecular order in the neighbouring layer is not deformed. We consider three types of structure: twisted, mixed and uniform anticlinic antiferroelectric.

Twisted structures mediate synclinic ferroelectric order on both surfaces with SmC_AP_A structure in the bulk. The mixed structure connects synclinic ferroelectric order on one surface with bulk SmC_AP_A. This bulk SmC_AP_A continues up to the second surface. The uniform SmC_AP_A structure finishes at surfaces without change. We calculate the energies of those structures and discuss their conditions of realization in order to explain the observations in [12].

This contribution is organized as follows. After short review of experimental observations in section 2, general energy considerations are treated in section 3. A model potential of the interaction of neighbouring layers using the analogy with the method given in [13, 14] for antiferroelectric smectic liquid crystals with rod-like molecules is proposed. Then the elasticity of biaxial nematics [15] is adopted to simply take into account the energy of twist deformation of the B_2 phase. As for the polar term in the elastic free energy, the linear term in gradients of polarization, proposed in [16, 17], is added. This term transforms into a surface term, which can be included in the surface anchoring energy [18–20].

The twisted solution connecting synclinic ferroelectric and anticlinic antiferroelectric structures is proposed in section 4. The energies of the twisted, mixed and uniform structures are estimated in section 5. The comparison with experimental observations in section 6 gives estimates of the order of model parameters as anchoring energies and the interaction energy of molecules leading to an anticlinic order.

2. Experimental observations

Observations of the B_2 phase were performed in a material based on a central 1,3-phenylene unit with ester

---

*Corresponding author. Email: lejcekl@fzu.cz

Liquid Crystals
ISSN 0267-8292 print/ISSN 1366-5855 online © 2008 Taylor & Francis
http://www.tandf.co.uk/journals
DOI: 10.1080/02678290701744553

linkages and lateral methoxy groups near a central benzene ring (called 10WDVI in [11]) and in materials having an asymmetrical bent core with six phenyl rings, laterally substituted by a methoxy group (denoted by **4d** or 11BVID11 in [12]). When materials are cooled very slowly from the isotropic phase, two types of domain may appear simultaneously. In one domain the optical extinction in crossed polarizers along the smectic layer normal occurs. It is probably a structure composed of mesoscopic grains of SmC_AP_A of opposite handedness (chirality) [7, 11]. In the second type of domain the rotation of the polarized light plane is observed. We can consider that this domain has a twisted structure of molecular organization within the smectic layers [7, 9–12]. Observations of domains of uniform SmC_AP_A structures (green domains) and twisted structures (pink domains) for compounds 10WDVI [11] and 11BVID11 [12] are shown in figures 1(a) and (b), respectively.

This observed twisted structure is the consequence of strong polar anchoring on the surfaces. The polar anchoring leads to the synclinic ferroelectric order on surfaces. The preferred orientations of molecular polarizations on the upper and lower surfaces are opposite as the glass plates used for sample preparation are the same.

As both types of structure can coexist, one can conclude that the structures have very similar energies.

3. Energy considerations

In this section, the different energies necessary for estimating the energies of the B_2 structures are outlined. After a general description of molecular orientation in section 3.1 the free energy of the anticlinic antiferroelectric B_2 phase as the basic state is proposed in section 3.2. Then the surface anchoring energy is taken in account (section 3.3). As the other domains of anticlinic antiferroelectric structure treated in this contribution are twisted modifications of basic state, the simplified twist deformation is introduced in section 3.4.

3.1 *Molecular orientation in layers*

The orientation of the bent-shaped molecules in layers can be described by three Eulerian angles θ, ϕ and ψ with respect to the coordinate system with x- and y-axes parallel to the smectic layers and the z-axis normal to the plane of smectic layers (figure 2). Let the unit vector in the direction of layer normal (positive direction of the z-axis) be denoted by $\vec{N}$. The angle θ describes the tilt of a long molecular axis, the orientation of which coincides with molecular unit director $\vec{n}$. The azimuthal angle ϕ characterizes the director rotation around the z-axis. (In figure 2 the rotation of the director $\vec{n}$ on the surface of

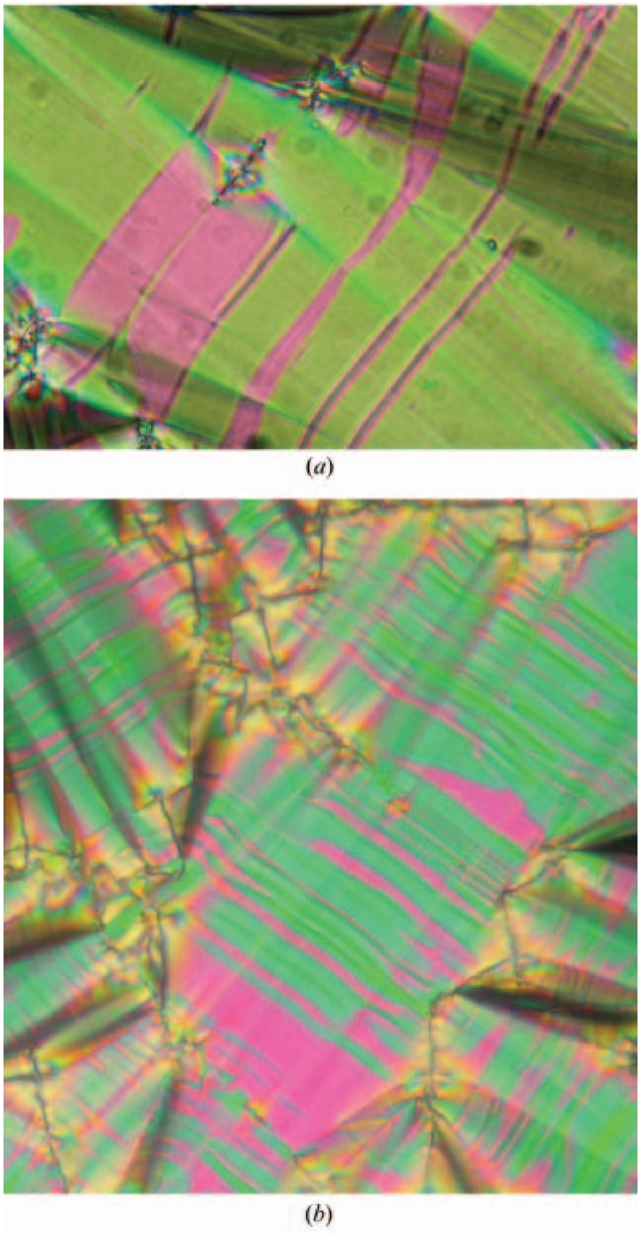
(*a*)

(*b*)

Figure 1. Planar textures in B_2 phases: (a) compound 10WDVI and (b) compound 11BVID11. Pink domains in (a) and (b) rotate the polarized light thus exhibiting twisted structures, while green domains are uniform structures.

the cone is characterized by ϕ, the angle between the x- and x'-axes.) Finally, the angle ψ describes the rotation of the plane containing the bent-shaped molecule around the $\vec{n}$-director axis. This rotation is measured starting from the x'-axis.

As a bent-shaped molecule lies in the plane that also contains the molecular dipole moment, the direction of which can be denoted as $\vec{p}$ perpendicular to $\vec{n}$, the angle ψ also describes the rotation of $\vec{p}$. Denoting by $\vec{m}$ the

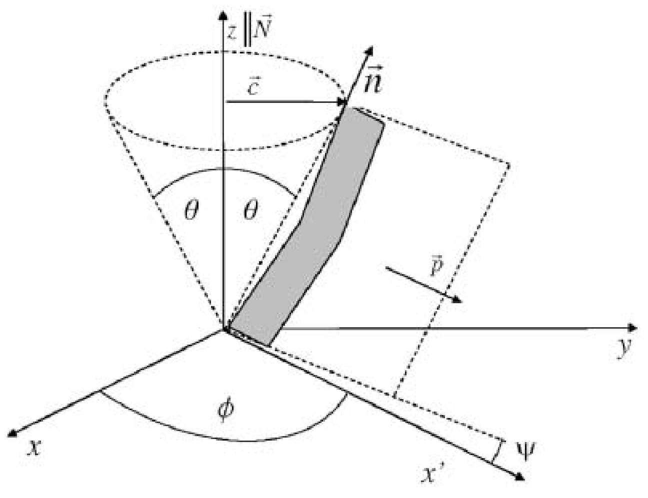

Figure 2. Bent-shaped molecule (a grey bent-shaped object) and the coordinate system.

unit vector perpendicular to the plane containing a bent-shaped molecule (both $\vec{p}$ and $\vec{n}$ are situated in this plane) we have three orthogonal unit vectors characterizing the molecular position with respect to the coordinate system (x, y, z). Those three vectors can be expressed using Eulerian angles as in [15]:

$$\begin{aligned}\vec{p} &= (\cos\theta\cos\phi\cos\psi - \sin\phi\sin\psi, \cos\theta\sin\phi\cos\psi \\ &\quad + \cos\phi\sin\psi, -\sin\theta\cos\psi) \\ \vec{m} &= (-\cos\theta\cos\phi\sin\psi - \sin\phi\cos\psi, -\cos\theta\sin\phi\sin\psi \\ &\quad + \cos\phi\cos\psi, \sin\theta\sin\psi) \\ \vec{n} &= (\sin\theta\cos\phi, \sin\theta\sin\phi, \cos\theta).\end{aligned} \tag{1}$$

When no layer deformations are considered, for which the vector $\vec{N}$ normal to layers is constant (i.e. smectic layers are well parallel and the molecular tilt angle θ is constant), it is more suitable to describe the system with three vectors: vector $\vec{N}$; director $\vec{c} = (\cos\phi, \sin\phi, 0)$, which is the projection of the director $\vec{n}$ onto the plane (x, y) of smectic layers; and vector $\vec{b}$ perpendicular to $\vec{c}$ and $\vec{N}$. The orientation of the three vectors $\vec{c}$, $\vec{b}$ and $\vec{N}$ with respect to the coordinate system (x, y, z) forms either a right-handed or left-handed triangle defining (+) or (−) layer chirality as discussed in [2, 3]. Within this contribution, we further suppose that the vector $\vec{p}$ is situated in smectic layers as in smectic C* with elongated molecules [8]. Then the vector of spontaneous polarization $\vec{p}$ is parallel to $\vec{b}$.

Note that generally the polarization vector $\vec{p}$ and vector $\vec{m}$ can rotate around the axis defined by director $\vec{n}$ (figure 2). This rotation leads to the change of chirality of the smectic layer in the sense of [2, 3].

In order to describe the anticlinic antiferroelectric state of the B_2 phase we use the bilayer model as proposed in [13, 14] for the case of antiferroelectric liquid crystals with elongated molecules. Let us suppose that the molecular orientation is characterized by angles ϕ_1 and ψ_1 in odd-numbered layers and ϕ_2 and ψ_2 in even-numbered layers. Then we can define vectors $\vec{c}_1 = (\cos\phi_1, \sin\phi_1, 0)$, $\vec{c}_2 = (\cos\phi_2, \sin\phi_2, 0)$, $\vec{p}_1$ and $\vec{p}_2$ using expression (1) with angles ϕ_1, ψ_1 and ϕ_2, ψ_2, respectively. According to Orihara and Ishibashi [13] let us introduce vectors

$$\vec{c}_+ = (\vec{c}_1 + \vec{c}_2)/2 \quad \text{and} \quad \vec{c}_- = (\vec{c}_1 - \vec{c}_2)/2 \tag{2a}$$

and

$$\vec{p}_+ = (\vec{p}_1 + \vec{p}_2)/2 \quad \text{and} \quad \vec{p}_- = (\vec{p}_1 - \vec{p}_2)/2. \tag{2b}$$

For $\vec{c}_+ = \vec{c}_1 = \vec{c}_2$ and $\vec{c}_- = 0$, i.e. for $\phi_1 = \phi_2$, we deal with synclinic molecular orientation, $\vec{c}_+ = 0$ and $\vec{c}_- = \vec{c}_+ = -\vec{c}_2$, i.e. for $\phi_1 = \phi_2 + \pi$, defines anticlinic molecular orientation. Therefore, vectors $\vec{c}_+$ and $\vec{c}_-$ are useful to denote synclinic and anticlinic molecular structures.

For a ferroelectric structure it is $\vec{p}_+ = \vec{p}_1 = \vec{p}_2$ (and $\vec{p}_- = 0$). For a synclinic molecular configuration such a structure can be realized if $\psi_1 = \psi_2 = \psi$. For the anticlinic configuration, the ferroelectric phase can be realized only when polarizations in neighbouring layers are situated in smectic layers, i.e. for angles $\psi_1 = \psi_2 = \pi/2$.

The antiferroelectric configuration is then characterized by $\vec{p}_+ = 0$ and $\vec{p}_- = \vec{p}_1 = -\vec{p}_2$. The synclinic antiferroelectric configuration is realized for $\psi_1 = \psi$ and $\psi_2 = \psi + \pi$ with arbitrary ψ. The anticlinic configuration leads to antiferroelectric polarizations for $\psi_1 = \psi_2 = \pi/2$ only, i.e. when polarizations in neighbouring layers are situated in smectic layers, similarly as in the case of the anticlinic ferroelectric configuration.

3.2 *The free energy of the non-deformed anticlinic antiferroelectric B_2 phase*

In order to express the preference of liquid crystals to organize themselves into anticlinic antiferroelectric structures we use the energy terms given in [13]. These non-gradient terms in free-energy density were used in [13] for a general discussion of transitions between possible structures with temperature:

$$\begin{aligned}w_C = {}& \frac{\alpha_-}{2}\vec{c}_-^{\,2} + \frac{\alpha_+}{2}\vec{c}_+^{\,2} + \frac{\beta_-}{4}\vec{c}_-^{\,4} + \frac{\beta_+}{4}\vec{c}_+^{\,4} + \frac{\gamma_{c1}}{2}\vec{c}_+^{\,2}\vec{c}_-^{\,2} \\ & + \frac{\gamma_{c2}}{2}(\vec{c}_-\vec{c}_+)^2,\end{aligned} \tag{3}$$

with $\vec{c}_+^2 = \frac{1}{2}(1 + \cos(\phi_1 - \phi_2))$ and $\vec{c}_-^2 = \frac{1}{2}(1 - \cos(\phi_1 -$

ϕ_2)). Expression (3) is written using parameters $\vec{c}_+$ and $\vec{c}_-$ only supposing with [8] that the vector of spontaneous polarizations $\vec{p}_1$ is perpendicular to director $\vec{c}_1$ and $\vec{p}_2$ is perpendicular to $\vec{c}_2$ and that all of those vectors lie in the smectic layer planes.

The interaction terms such as $(\vec{c}_+\vec{p}_+)^2$, $(\vec{c}_-\vec{p}_-)^2$, $(\vec{c}_+\vec{p}_-)^2$ and $(\vec{c}_-\vec{p}_+)^2$ which could be present in (3) are either zero or they are equivalent to terms of the type $\vec{c}_+^2\vec{c}_-^2$.

In general, the parameters α_+ and α_- depend on temperature. In this contribution we suppose that we are already in the temperature range where the antiferroelectric anticlinic structure can be realized. Thus, we take α_+ and α_- to be fixed.

The condition of extreme of (3) with respect to angles ϕ_1 and ϕ_2 gives $\phi_1=\phi_2$, $\phi_1=\phi_2+\pi$ and $\cos(\phi_1-\phi_2)=[2(\alpha_- - \alpha_+)+(\beta_- - \beta_+)]/(\beta_- + \beta_+ - 2\gamma_{c1})$.

In order to obtain a simple potential, we ask for a minimum of (3) in the antiferroelectric anticlinic configuration and a maximum in the ferroelectric state. Then the energy of the configuration $\phi_1=\phi_2+\pi$ should correspond to the minimum and $\phi_1=\phi_2$ to the maximum of energy with no other extreme. The parameters in (3) should satisfy the relation

$$2\alpha_- + \beta_- < 2\alpha_+ + \beta_+ .$$

In order to simplify our further analysis and to obtain a simple one-constant approximation of this potential, we take $\alpha_+=\beta_+=0$. This means that the energy of the ferroelectric synclinic configuration is fixed as zero. As $|(2\alpha_- + \beta_-)/(\beta_- - 2\gamma_{c1})| = |\cos(\phi_1-\phi_2)| \leq 1$, we expect $0<2\gamma_{c1}<\beta_-$ and we neglect γ_{c1} with respect to β_- for simplicity. We also take, in accordance with [14], $\gamma_{c2}=0$.

Coefficient $\beta_->0$ stabilizes the energy. The coefficient α_- is negative in the antiferroelectric state in order to decrease the energy of the antiferroelectric state with respect to the ferroelectric state. A simplified one-constant approximation of w_C can then be obtained, for example, by taking $\alpha_-/\beta=-1$. It is an arbitrary choice defining our model potential. Then $\cos(\phi_1-\phi_2)=-1$, which gives the already determined extreme.

Then the energy w_C takes a model form:

$$\begin{aligned} w_C &= \frac{\beta_-}{2}\left(-1+\frac{\vec{c}_-^2}{2}\right)\vec{c}_-^2 \\ &= \frac{\beta_-}{16}(-1+\cos(\phi_1-\phi_2))(3+\cos(\phi_1-\phi_2)). \end{aligned} \tag{4}$$

The minimum energy $w_C=-\beta_-/4$ of (4) corresponds to the anticlinic antiferroelectric structure ($\phi_1=\phi_2+\pi$) while synclinic ferroelectric structure ($\phi_1=\phi_2$) has, by definition, the energy $w_C=0$.

3.3 *Surface anchoring energy*

In models of real B_2 structure it is important to know how the molecules are anchored to the surface. This problem has already been discussed in [18]. For smectic layers perpendicular to sample surfaces the part of anchoring energy W_p describing the interaction of spontaneous polarization with surfaces can be expressed similarly as in the case of antiferroelectric liquid crystals proposed in [19]:

$$W_P = -\gamma_1\left(\vec{N}_S.\vec{p}_+\right)^2 + \gamma_2\left(\vec{N}_S.\vec{p}_+\right) - \gamma_3\left(\vec{N}_S.\vec{p}_-\right)^2. \tag{5}$$

In this expression, the external normal to sample surface is denoted by $\vec{N}_S$ (parallel or antiparallel to the x-axis) and parameters γ_1, γ_2 and γ_3 are the anchoring constants or anchoring energies per unit surface. They describe the polar interactions of the liquid crystal with the sample surfaces. The origin of such interactions is connected with the creation of polarization terms in a similar manner as in nematic liquid crystals, as discussed thoroughly in [21].

The first term in (5) characterizes the non-polar anchoring and it attains a minimum value for $\vec{p}_+$ parallel or antiparallel to $\vec{N}_S$. The second term expresses the polar anchoring of molecules. Note that the bulk polar term $\operatorname{div}\vec{p}_+$, which can exist in the polar B_2 phase [16, 17], adds to this surface term. Let us suppose that the preferable orientation for $\vec{p}_+$ directs to the inside of the sample. Then this term has the sign (+) in (5).

The analogous term, proportional to $\left(\vec{N}_s.\vec{p}_-\right)$, is not invariant with respect to translation for a layer thickness and changes sign depending on the choice of neighbouring layers forming a bilayer. For this reason this term is not considered as in [19].

The third term describes the antiferroelectric interaction of molecules with surfaces. The anchoring energy (5) differs for ferroelectric and antiferroelectric anchoring. For example, when the ferroelectric anchoring is preferred, the anchoring energy (5) should be minimal for ferroelectric and maximal for antiferroelectric anchoring. The anchoring energy (5) corresponding to ferroelectric anchoring can be evaluated with $\left(\vec{N}_s.\vec{p}_+\right)=-1$ and $\left(\vec{N}_s.\vec{p}_-\right)=0$ as $W_p^{FE}=-(\gamma_1+\gamma_2)$. The energy of antiferroelectric anchoring W_p^{AF} can be obtained using $\vec{p}_+=0$ and $\left(\vec{N}_s.\vec{p}_-\right)^2=1$ as $W_p^{AF}=-\gamma_3$.

The condition of surface energy minimum for ferroelectric anchoring, $W_p^{FE}<W_p^{AF}$, leads to inequality $\gamma_1+\gamma_2>\gamma_3$. This means that for anchoring energy (5) the antiferroelectric anchoring is always unfavourable as compared with ferroelectric and non-polar anchoring.

The anchoring energy (5) describes the interaction of molecular polarization with surfaces. As shown in [18], other anchoring terms are possible which can prefer the plane of bent-shaped molecules to be either parallel or perpendicular to the surface. Such terms can be formally the same as those in (5), however with $\vec{p}$ changed to $\vec{c}$, $\gamma_4\left(\vec{N}_s.\vec{c}_+\right)+\gamma_5\left(\vec{N}_s.\vec{c}_+\right)^2+\gamma_6\left(\vec{N}_s.\vec{c}_-\right)^2$.

As we assume the surface order to be either synclinic or anticlinic with $\vec{c}$ directors parallel to surfaces, we take $\gamma_4=0$, $\gamma_5>0$ and $\gamma_6>0$. Then we propose the total anchoring energy W_{A} in the form:

$$\begin{aligned} W_{\mathrm{A}} = & -\gamma_1\left(\vec{N}_{\mathrm{S}}.\vec{p}_+\right)^2+\gamma_2\left(\vec{N}_{\mathrm{S}}.\vec{p}_+\right)-\gamma_3\left(\vec{N}_{\mathrm{S}}.\vec{p}_-\right)^2 \\ & +\gamma_5\left(\vec{N}_{\mathrm{S}}.\vec{c}_+\right)^2+\gamma_6\left(\vec{N}_S.\vec{c}_-\right)^2. \end{aligned} \tag{6}$$

3.4 *Approximated twist deformation energy*

The bulk basic state of the B_2 phase is the uniform anticlinic antiferroelectric structure. On surfaces, the ferroelectric anchoring with synclinic order can be realized owing to anchoring. The connection of bulk anticlinic antiferroelectric structure with synclinic ferroelectric structure near the surfaces requires twist in at least one layer while the neighbouring layer can, for example, be uniform.

In order to describe a twist deformation of molecules in non-deformed smectic layers (the tilt angle θ is constant), the elasticity of biaxial nematics (given, e.g., in [15]) could be helpful. However, in the elastic energy of [15] a one-constant approximation was assumed with the elastic constant *K*. We rewrite the expression of the biaxial nematic elasticity given in [15] for neighbouring layers where the molecular orientations are described by angles ϕ_1 and ψ_1 and ϕ_2 and ψ_2.

As molecular polarizations lie in smectic layers, angles ψ_1 and ψ_2 are $\psi_1=\psi_2=\pi/2$. The angles ϕ_1 and ϕ_2 depend on one variable x oriented along the sample thickness. In one-constant approximation, Mathematica [22] gives simply

$$f_d=\frac{K}{4}\left[\left(\frac{\partial\phi_1}{\partial x}\right)^2+\left(\frac{\partial\phi_2}{\partial x}\right)^2\right]. \tag{7}$$

This expression describes the molecular rotation on the surfaces of cones (figure 1) along the sample thickness in neighbouring layers. Expression (7) is the simplest deformation energy, which can be also obtained from the deformation free-energy density of non-chiral smectic layers with elongated molecules assuming that their independent molecular rotations are in neighbouring layers.

The only polar term used in our model is the term $\operatorname{div}\vec{p}_+$ already added to the anchoring energy in section 3.3.

4. Twist deformation of the B$_2$ structure in a finite sample

In this section we consider the twisted structure of bent-shaped molecules organized in smectic layers perpendicular to sample surfaces. If sample surfaces are perpendicular to the *x*-axis, we obtain a thickness profile of the twisted structure in the sample.

We look for extremes of the energy

$$\int_{-\frac{d}{2}}^{+\frac{d}{2}}(f_d+w_c)dx,$$

where *d* is the sample thickness. Variation with respect to angles ϕ_1 and ϕ_2 gives (using the method in [22]) two equilibrium equations:

$$\frac{\partial^2\phi_1}{\partial x^2}+\frac{4}{\zeta^2}\cos^3\left(\frac{\phi_1-\phi_2}{2}\right)\sin\left(\frac{\phi_1-\phi_2}{2}\right)=0 \tag{8a}$$

and

$$\frac{\partial^2\phi_2}{\partial x^2}-\frac{4}{\zeta^2}\cos^3\left(\frac{\phi_1-\phi_2}{2}\right)\sin\left(\frac{\phi_1-\phi_2}{2}\right)=0. \tag{8b}$$

The parameter $\zeta=\sqrt{4K/\beta_-}$ characterizes the length where most of the twist deformation is concentrated.

Boundary conditions are supposed to be of the form $\phi_1(-d/2)=c_d$, $\phi_2(-d/2)=-\pi/2$ on the lower surface and $\phi_1(d/2)=\pi/2$, $\phi_2(d/2)=c_h$ on the upper surface. The parameters c_d and c_h are at intervals $(-\pi/2,\ \pi/2)$ and their combination can give either twisted, uniform or intermediate solutions.

Equations (8) simplify for ferroelectric ($\phi_1=\phi_2$) or antiferroelectic order ($\phi_1=\phi_2+\pi$) to the form $\partial^2\phi_2/\partial x^2=0$. However, we look for another solution which connects the bulk anticlinic antiferroelectric structure with surface synclinic ferroelectric order. Such a solution of (8) can be composed from solutions in the lower and upper parts of the sample.

In the lower part of the sample, $x\in(-d/2,0)$, where ϕ_2 is fixed constant the equation (8a) is valid only. Then the solution in this part of the sample can be summarized as

$$\phi_1(x)=2\arctan\left(\frac{Q_d}{-1+Q_d}\right) \quad \text{and} \quad \phi_2(x)=-\frac{\pi}{2}, \tag{9a}$$

with

$$Q_d=\frac{1}{2}\left(-\frac{x}{\zeta}-\frac{d}{2\zeta}+\frac{2\tan(c_d/2)}{-1+\tan(c_d/2)}\right).$$

Solution (9a) describes molecules in one layer rotating at the lower part of the sample while the neighbouring layer keeps the constant orientation from the lower surface to the sample centre.

In the upper part of the sample, $x\in(0,d/2)$, the function ϕ_1 is chosen to be constant and only equation (8b) is valid. The solution in this part of the sample is then in the form:

$$\phi_1(x)=\frac{\pi}{2} \quad \text{and} \quad \phi_2(x)=2\arctan\left(\frac{-Q_h}{Q_h-1}\right), \tag{9b}$$

with

$$Q_h=\frac{1}{2}\left(\frac{x}{\zeta}-\frac{d}{2\zeta}+\frac{2\tan(c_h/2)}{1+\tan(c_h/2)}\right).$$

Solution (9b) is valid for the upper part of the sample and describes molecules with constant orientation in one layer and molecules rotating from the sample centre up to the surface in the neighbouring layer.

A solution over the whole sample thickness is composed of solutions in the lower and upper half of the sample connected at $x=0$. While the first derivatives of the solutions are continuous at the sample centre, i.e. it is $\partial\phi_1(x)/\partial x|_{x=0}=\partial\phi_2(x)/\partial x|_{x=0}=0$ at $x=0$, solutions are continuous in limit, i.e. $\phi_1(x=0)\rightarrow\pi/2$ and $\phi_2(x=0)\rightarrow-\pi/2$ when $d\gg 2\zeta$. In this sense our solutions are approximate. However, the advantage of this approximation is that the solutions (9) are expressed in the analytic form.

The elastic energy $W_{\mathrm{el}}^{\mathrm{T}}$ (per unit surface of the (y, z) -plane) stored in the structure described by the solution (9) can be evaluated as

$$W_{\mathrm{el}}^{\mathrm{T}}=\int_{-\frac{d}{2}}^{+\frac{d}{2}}(f_d+w_c)dx=$$

$$\frac{K}{4}\int_{-\frac{d}{2}}^{0}\left[\left(\frac{\partial\phi_1}{\partial x}\right)^2+\frac{1}{\zeta^2}(1+\sin\phi_1)(-3+\sin\phi_1)\right]dx$$

$$+\frac{K}{4}\int_{0}^{\frac{d}{2}}\left[\left(\frac{\partial\phi_2}{\partial x}\right)^2+\frac{1}{\zeta^2}(-1+\sin\phi_2)(3+\sin\phi_2)\right]dx$$

$$\begin{aligned}=&\frac{K}{\zeta}\left(\arctan\left(\frac{1-\tan(c_d/2)}{1+\tan(c_d/2)}\right)-\arctan\frac{1-\tan(c_d/2)}{(1+t)-(t-1)\tan(c_d/2)}\right.\\&\left.+\frac{t\left(-t^2-1-\cos^2c_d+(t/2)\cos c_d(-5+\sin c_d)+\left(t^2-1\right)\sin c_d\right)}{t^2+2+2t\cos c_d-t^2\sin c_d}\right)\\&-\frac{K}{\zeta}\left(\arctan\left(\frac{1+\tan(c_h/2)}{-1+\tan(c_h/2)}\right)+\arctan\frac{1+\tan(c_h/2)}{(1+t)+(t-1)\tan(c_h/2)}\right.\\&\left.+\frac{t\left(t^2+1+\cos^2c_h+(t/2)\cos c_h(5+\sin c_h)+\left(t^2-1\right)\sin c_h\right)}{t^2+2+2t\cos c_h+t^2\sin c_h}\right).\end{aligned} \tag{10}$$

The parameter t is defined as $t=d/2\zeta$.

5. Models of B$_2$ structures and their energies

In this section we compare the energies of three B$_2$ structures. Inspection of expression (10) shows immediately that there is only one minimum of the elastic bulk energy $W_{\mathrm{el}}^{\mathrm{T}}$ for $c_d=\pi/2$ and $c_h=-\pi/2$. This structure corresponds to the uniform anticlinic antiferroelectric structure with no twist because solutions (9) reduce to $\phi_1(x)=\pi/2$ and $\phi_2(x)=-\pi/2$. Its energy $W_{\mathrm{el}}^{\mathrm{T}}$ can be obtained from (10) as $-2Kt/\zeta$. However, the possibility of observed coexistence of uniform anticlinic antiferroelectric structure together with twisted structure as presented in section 2 requires a discussion of the bulk elastic energy (10) and the surface anchoring energy (6), i.e. $W_{\mathrm{el}}^{\mathrm{T}}+W_{\mathrm{A}}$. Then the existence of other energy minima can arise.

So we study, using [22], extreme conditions $\partial\left(W_{\mathrm{el}}^{\mathrm{T}}+W_{\mathrm{A}}\right)/\partial c_d=0$ and $\partial\left(W_{\mathrm{el}}^{\mathrm{T}}+W_{\mathrm{A}}\right)/\partial c_h=0$. In order to work with non-dimensional expressions, both energies can be multiplied by d/K. Then the surface anchoring energy $W_{\mathrm{A}}d/K$ will be expressed at the upper and lower surfaces as

$$\begin{aligned}\frac{W_{\mathrm{A}}d}{K}=&-\frac{g_1}{4}\left[(1-\sin c_d)^2+(1+\sin c_h)^2\right]\\&-\frac{g_2}{2}[2-\sin c_d+\sin c_h]\\&-\frac{g_3}{4}\left[(1+\sin c_d)^2+(1-\sin c_h)^2\right]\\&+\frac{(g_5+g_6)}{4}\left[\cos^2c_d+\cos^2c_h\right],\end{aligned} \tag{11}$$

with $g_i=\gamma_i d/K$ ($i=1$, 2, 3, 5, 6). The positions of the energy minima are controlled principally by parameters g_5 and g_6. When $g_5\gg t$ and $g_6\gg t$ and $|-g_2+2g_3|<g_5+g_6$, energy minima are situated very close to $c_d=\pm\pi/2$, $c_h=\pm\pi/2$ and the energy maximum is situated near $c_d=c_h=0$.

In the following we estimate the energies of structures at the minima and compare them.

5.1 *Twisted structure*

The general solution leading to a twisted structure was described in section 4 and is shown schematically in figure 3(a). When the anchoring is strong enough to keep the director parallel to the surfaces, then this structure can be realized nearly exactly for $c_d = -\pi/2$ and $c_h = \pi/2$. The energy W^{T} of this structure (per unit surface) can be determined using (10) and (11) as

$$W^{\mathrm{T}} = -2(\gamma_1 + \gamma_2) - \frac{2K}{\zeta}\left[t\left(1 - \frac{1}{1+t^2}\right) - \arctan t\right]. \tag{12}$$

5.2 *Uniform anticlinic antiferroelectric structure*

Another structure is the uniform anticlinic antiferroelectric structure in the whole sample (figure 3(b)). Its energy W^{AA} follows from (10) and (11) by taking $c_d = \pi/2$ and $c_h = -\pi/2$:

$$W^{\mathrm{AA}} = -2\gamma_3 - \frac{\beta\_d}{4} = -2\gamma_3 - \frac{2K}{\zeta}t. \tag{13}$$

5.3 *Mixed structures*

The mixed structure twisted at the lower part and uniform anticlinic antiferroelectric in the upper part of the sample is shown in figure 3(c). This solution is characterized by parameters $c_d = -\pi/2$ and $c_k = -\pi/2$.

Then the energy W^{AT} of the mixed structure can be expressed in the form

$$W^{\mathrm{AT}} = -\frac{K}{\zeta}\left[t\left(1 - \frac{1}{1+t^2}\right) - \arctan t\right] - (\gamma_1 + \gamma_2 + \gamma_3) - \frac{K}{\zeta}t. \tag{14}$$

The other mixed structure is twisted at the upper part of the sample and it is uniform at the lower part of the sample. Such a solution is characterized by parameters $c_d = \pi/2$ and $c_h = \pi/2$.

6. Comparison with observations

Experimental observations described in section 2 can distinguish between non-twisted structures and twisted structures in samples about 4 μm thick. Therefore, we can assume that the energies of twisted and non-twisted structures at this sample thickness are comparable, i.e. $W^{\mathrm{T}} \approx W^{\mathrm{AA}}$. Using (12) and (13) we obtain the relation

$$(\gamma_1 + \gamma_2 - \gamma_3) \approx \frac{K}{\zeta}\left[\frac{t}{1+t^2} + \arctan t\right]. \tag{15}$$

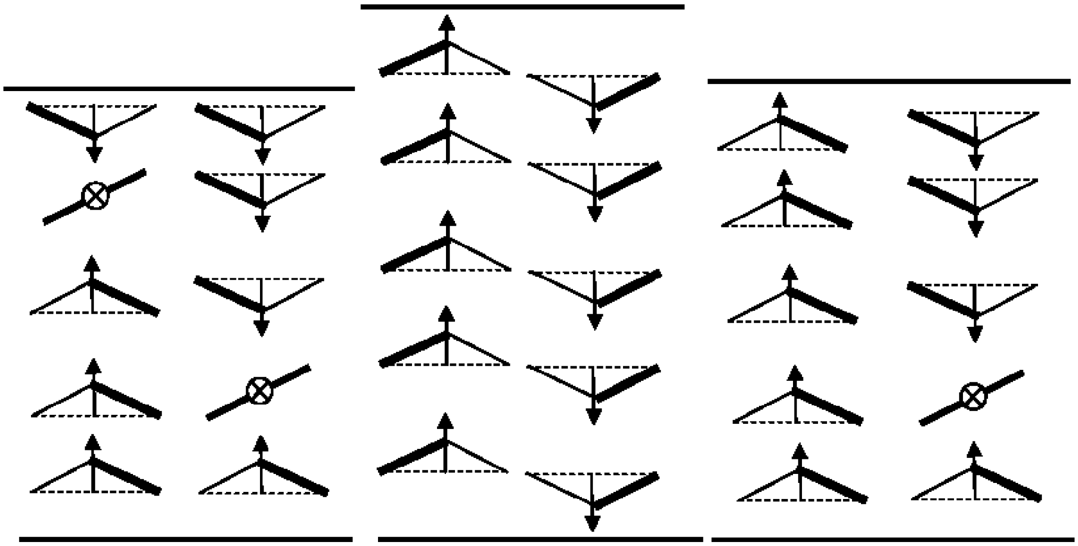

(*a*) (*b*) (*c*)

Figure 3. Possible structures in the B_2 phase. Smectic layers perpendicular to sample surfaces are observed from the side. Molecular orientation in neighbouring layers is represented by triangles where the thicker line corresponds to the arm of the bent-shaped molecule inclined towards the observer. The molecular $\vec{n}$ director is situated on the surface of a cone as in figure 2, dashed lines indicate the positions of the director on the cone projected onto the plane of the figure. Molecular spontaneous polarizations are depicted by arrows, the length and orientations of which correspond to the projection of polarization onto the plane of the figure. (a) Connection of $\mathrm{SmC_SP_F}$ structures near the upper and lower surfaces with $\mathrm{SmC_AP_A}$ structure in the sample bulk. Rotation of bent-shaped molecules occurred in one layer while molecules in the neighbouring layer are fixed. (b) Uniform $\mathrm{SmC_AP_A}$ structure. (c) Mixed structure with twisted deformation near the upper surface and uniform $\mathrm{SmC_AP_A}$ structure in the sample bulk and near the upper surface.

However, when (15) is satisfied, this model immediately gives the relation $W^{\mathrm{T}} \approx W^{\mathrm{AT}} \approx W^{\mathrm{AA}}$. Therefore, without an electric field all three structures have the same energies. The right-hand side of (15) is principally the energy of twist deformation which is concentrated on the length ζ.

When $d > \zeta$, the right-hand side of (15) approaches a constant value with increasing sample thickness d. Thus, the right-hand side of (15) does not change quickly with d. Therefore, for a given material a sample thickness exists for which the three structures of B_2 phase mentioned above can be realized in the same sample.

Let us estimate the order of anchoring energies. We used the estimate of the elastic constant K taken as for the nematic phase of rod-like molecules, i.e. $K \approx 10^{-11}\,\mathrm{J\,m^{-1}}$ (see [20]).

As for the value of β_-, its value given for different rod-like liquid crystalline materials in [24] will be taken in this contribution as $\beta_- \approx 10^5\,\mathrm{J\,m^{-3}}$. Then $\zeta \approx 0.02\,\mu\mathrm{m}$, it is $\zeta < d$ as the sample thickness used in observations [12] is $d = 4\,\mu\mathrm{m}$. The parameter $t = d/2\zeta$ is about $t \approx 100$.

Let us assume that the polar anchoring energy is the dominant term as compared with non-polar and antiferroelectric anchoring terms. For simplicity let us suppose $\gamma_1 \approx \gamma_3 \approx 0$. The formula (15) then determines the anchoring energy $\gamma_2 \approx 10^{-3}\,\mathrm{J\,m^{-2}}$. This value of polar anchoring energy γ_2 corresponds to the strong anchoring [23].

As for the values of γ_5 and γ_6 we suppose $\gamma_5 \approx \gamma_6$. Using [22] we adjust the energy minima to be situated at $c_d = \pm\pi/2$, $c_h = \pm\pi/2$ using the value $\gamma_5 \approx 2 \times 10^{-3}\,\mathrm{J\,m^{-2}}$. Such a value gives a strong preference for the directors $\vec{c}_1$ and $\vec{c}_2$ to be parallel to the surfaces and also perpendicular to molecular polarizations (without an external electric field) [8]. In figure 4 the total energy $W_{\mathrm{T}} d/K = \left(W_{\mathrm{el}}^{\mathrm{T}} + W_{\mathrm{A}}\right) d/K$ is plotted using the above-mentioned parameters.

However, the model parameter $\zeta \approx 0.02\,\mu\mathrm{m}$ expressing the length over which the structure rotates is smaller as compared with the optical wavelengths. When ζ is increased, say up to $\zeta \approx 0.2\,\mu\mathrm{m}$, the value of β_- decreases to $\beta_- \approx 10^3\,\mathrm{J\,m^{-3}}$ (when the elastic constant K is fixed). In such a case (supposing again $\gamma_1 \approx \gamma_3 \approx 0$ and $\gamma_5 \approx \gamma_6$) anchoring energies γ_2 and γ_5 are smaller: $\gamma_2 \approx 7 \times 10^{-5}\,\mathrm{J\,m^{-2}}$, $\gamma_5 \approx 0.5 \times 10^{-3}\,\mathrm{J\,m^{-2}}$. However, the order of elastic constant K in smectic phases of bent-shaped molecules could be greater as compared with the nematic phase of rod-like molecules. Then, for given ζ the parameter β_- will also be greater.

Our model permits the coexistence of three structures while observations report only twisted and uniform anticlinic antiferroelectric domains, the mixed domains not being perceived. The reason might be their low optical contrast against the uniform domains, as in the mixed structure the twist does not occur in all smectic layers. The optical contrast of the above-mentioned structures in the B_2 phase can be also dependent on the length ζ where the twist takes place.

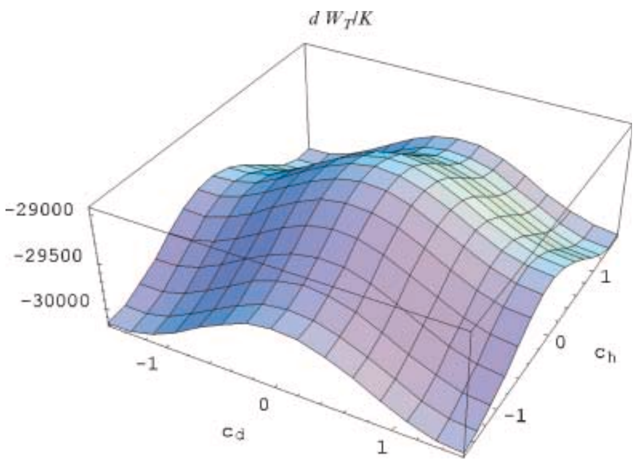

Figure 4. 3D schematic plot of the elastic and anchoring energy $d\ W_{\mathrm{T}}/K = \left(W_{\mathrm{el}}^{\mathrm{T}} + W_{\mathrm{A}}\right)$ as a function of surface $\vec{c}$-director orientations c_d and c_h on the lower and upper sample surfaces, respectively. Energy minima are situated near $c_d = \pm\pi/2$ and $c_h = \pm\pi/2$.

7. Conclusions

In the present contribution we treat the relatively thin sample where a competition between bulk and surface energies is important.

Therefore, two structures may be observed [12] without an applied external electric field in the form of domains differing in optical contrast:

1. a twisted structure;
2. domains of uniform chiral anticlinic antiferroelectric structures $\mathrm{SmC_AP_A}$.

In this contribution we have constructed the model of twisted structure where $\mathrm{SmC_AP_A}$ structure, which prevails in the sample bulk, is influenced by surface anchoring. When the surface anchoring prefers the surface synclinic ferroelectric structure the anticlinic antiferroelectric bulk structure can be mediated to surface synclinic ferroelectric order by molecular rotation in one layer while the molecular order in the neighbouring layer is not deformed. The bulk energy of the twisted structure is higher with respect to uniform structure which leads to an increase in the energy of the structure owing to twist deformation and disorder of $\mathrm{SmC_AP_A}$. On the other hand, the total energy decreases with surface anchoring energy.

As the uniform anticlinic antiferroelectric structure $\mathrm{SmC_AP_A}$ is observed together with twisted structure, both structures should have comparable energies. Structure $\mathrm{SmC_AP_A}$ has the lower bulk energy but elevated anchoring energy owing to antiferroelectric order at the surfaces.

Moreover, the model shows that so-called mixed structures can exist together with twisted and SmC_AP_A structures. Mixed structures have synclinic ferroelectric order on one surface and uniform SmC_AP_A order in the bulk and near the other surface.

When twisted and uniform SmC_AP_A structures have similar energies, the energy of the mixed structure is also comparable to these energies. This can be seen from the investigation of the total energy having minima corresponding to those structures (figure 4). Barriers between minima are determined from the surface anchoring energies.

The optical contrast of the above-mentioned possible B_2 structures probably depends on the length ζ on which the twist is realized. For very short ζ the uniform SmC_AP_A structure prevails in all three structures. Therefore, all structures could have a similar contrast. When ζ is higher, the twisted structure starts to differ optically from the mixed and uniform SmC_AP_A structures. Finally, for ζ of the order of a micrometer, all three structures should be optically different. This hypothesis should, however, be verified in future observations.

We conclude that in this contribution we have proposed models of B_2 structures observed in [12]. Observations of [12] reflect both the choice of particular sample thickness and the material, which leads to the coexistence of the twisted and uniform anticlinic antiferroelectric structures. We hope that the present model opens the path to more detailed models of observed B_2 structures, namely structure deformations under an applied field.

Acknowledgement

This work was supported by grant No. 202/05/0431 from the Grant Agency of the Czech Republic.

References

[1] T. Niori, T. Sekine, J. Watanabe, T. Furukawa, H. Takezoe. *J. Mater. Chem.*, **6**, 1231 (1996).

[2] D.R. Link, G. Natale, R. Shao, J.E. Maclennan, N.A. Clark, E. Korblova, D.M. Walba. *Science*, **278**, 1924 (1997).

[3] R.A. Reddy, C. Tschierke. *J. Mater. Chem.*, **16**, 907 (2006).

[4] H. Takezoe, Y. Takanishi. *Jpn. J. Appl. Phys.*, **45(2A)**, 597 (2006).

[5] W. Weissflog, U. Dunemann, M.W. Schroder, S. Diele, G. Pelzl, H. Kresse, S. Grande. *J. Mater. Chem.*, **15**, 939 (2005).

[6] L. Kovalenko, M.W. Schroder, R.A. Reddy, S. Diele, G. Pelzl, W. Weissflog. *Liq. Cryst.*, **32**, 8571 (2005).

[7] V. Novotná, V. Hamplová, M. Kašpar, M. Glogarová, D. Pociecha. *Liq. Cryst.*, **32**, 1115 (2005).

[8] M. Nakata, R.-F. Shao, J.E. Maclennan, W. Weissflog, N.A. Clark. *Phys. Rev. Lett.*, **96**, 067802 (2006).

[9] M. Nakata, D.R. Link, F. Araoka, J. Thisayuka, Y. Takanishi, K. Ishikawa, J. Watanabe, H. Takezoe. *Liq. Cryst.*, **28**, 1301 (2001).

[10] F. Araoka, H. Hoshi, H. Takezoe. *Phys. Rev. E*, **69**, 051704 (2004).

[11] V. Novotná, V. Hamplová, M. Kašpar, M. Glogarová, K. Knížek, S. Diele, G. Pelzl, Ch. Jones, D. Coleman, N.A. Clark. *Liq. Cryst.*, **32**, 967 (2005).

[12] V. Novotná, M. Kašpar, V. Hamplová, M. Glogarová, L. Lejček, J. Kroupa, D. Pociecha. *J. Mater. Chem.*, **16**, 2031 (2006).

[13] H. Orihara, Y. Ishibashi. *Jap. J. Appl. Phys.*, **29**, L115 (1990).

[14] I. Muševič, R. Blinc, B. Žekš. *The Physics of Ferroelectric and Antiferroelectric Liquid Crystals*. World Scientific, Singapore (2000).

[15] S. Stallinga, G. Vertogen. *Phys. Rev. E*, **49**, 1483 (1994).

[16] N. Vaupotič, M. Čopič. *Phys. Rev. E*, **72**, 031701 (2005).

[17] H. Pleiner, P.E. Cladis, H.R. Brand. *Eur. Phys. J.*, **E20**, 257 (2006).

[18] J. Maclennan, N.A. Clark, D.M. Walba. *Phys. Rev. E*, **64**, 031706 (2001).

[19] J. Pavel, P. Gisse, H.T. Nguyen, Ph. Martinot-Lagarde. *J. Phys. II France*, **5**, 355 (1995).

[20] P.G. de Gennes, J. Prost. *The Physics of Liquid Crystals,* 2nd edition, Oxford University Press (1993).

[21] M.A. Osipov, T.J. Sluckin, S.J. Cox. *Phys. Rev. E*, **55**, 464 (1997).

[22] S. Wolfram. *Mathematica*. Cambridge University Press, Cambridge (1996).

[23] P. Oswald, P. Pieranski. *Nematic and Cholesteric Liquid Crystals*. Taylor & Francis, London (2005).

[24] F. Giesselmann. *Smectic A–C Phase Transitions in Liquid Crystals*. Shaker, Aachen (1999).